RAY-TRACING TECHNIQUES FOR MOBILE COMMUNICATIONS.

O. Gutiérrez, F. Saez de Adana, I. González, J. Pérez, M. F. Cátedra

Dprt. de Teoría de la Señal y Comunicaciones.

Escuela Politéctica, Universidad de Alcalá

28806 Alcalá de Henares (Spain)

Tel: +34918856724, Fax: +34918856724

e-mail: felipe.catedra@uah.es

ABSTRACT

In this paper an application for mobile communication of several ray-tracing techniques is presented. The techniques work in combination with deterministic propagation models based on GTD/UTD techniques. Several ray-tracing techniques are reviewed and some results applying one of them, the Angular Zeta Buffer (AZB) method for urban and indoor scenarios are shown, obtaining in all the cases good results comparing with measurements.

1. INTRODUCTION

For mobile communication, traditionally, propagation models based on empirical and semi-empirical models have been used. Several models for urban and rural environments have been developed and largely used [1]. However, when the traffic had increased the size of the cells has decreased (microcells, picocells) and these methods do not provide good predictions and deterministic models should be used.

A model based on Geometric Optics (GO), on Geometrical Theory of Diffraction (GTD) and on Uniform Theory of Diffraction (UTD) is presented. This is a ray-based method, the electric field at the observation points is calculated as the coherent sum of the fields associated with the rays that reach the points.

The propagation model requires a detailed information about the environment, which includes geometric and electromagnetic information of the obstacles, that are modeled by means of flat facets, each one of them with its own electromagnetic properties. In complex environments, like mobile communications scenarios, the principal difficulty of the GTD application is to solve ray-tracing. It consumes most of the simulation time. The shadowing problem is the most critical part of the ray tracing from a computational point of view. The problem is to determine if any facet of the model shadows a ray, that is the so-called intersection test.

The ray tracing techniques have been developed in the last 30 year in the world of computer graphics for visualization of complex scenarios [2-3]. Some of the acceleration ray-tracing techniques used for computer graphics can be used in combination with UHF propagation models for the reduction of the number of intersection tests in mobile communications environments. They are the Space Volumetric Partitioning (SVP), the Binary Space Partitioning (BSP) and the Angular Z-Buffer (AZB).

Some computer codes have been developed, using the propagation model and the AZB technique, for different environments. Computer codes FASPRO [4] and FASPRI [5] have been developed for the analysis of urban and indoor environments, respectively. This paper presents the electromagnetic basis of the application of GTD/UTD to the prediction of propagation in mobile communications implemented in those codes (Section 2) and a survey of the main ray-tracing acceleration techniques mentioned above showing the advantages of the AZB technique for our purposes (Section 3), whereas in [4] only the comparison between two ray tracing techniques were presented. Also, in Section 4, a validation of the results of both codes, compared with measurements is shown. Finally, the conclusions are outlined in Section 5

1054-4887 © 2000 ACES

2. GTD/UTD APPROACH

The electric field $\vec{E}_T$ created at an observation point by a source will be approximated by:

$$\vec{E}_T = \sum_{i=1}^{N} \vec{E}_i \tag{1}$$

where $\vec{E}_i$ represents the electric field due to each one of the ray-paths which connect the source with the observation: direct ray, reflected rays, diffracted rays, transmitted rays, reflected-diffracted rays, double-reflected rays, etc.

Each $\vec{E}_i$ term can be computed using the ray-tube formulation of GTD/UTD [6]:

$$\vec{E}(s) = \vec{E}(s=0)\sqrt{\frac{\rho_1\rho_2}{(\rho_1+s)(\rho_2+s)}}\exp(-j\beta s) \tag{2}$$

where s is distance to the reference point ($s=0$), $\vec{E}(s=0)$ is the electric field at the reference point and ρ_1, ρ_2 are the principal radii of curvature of the wavefront associated with the ray at the reference point. β is the free-space wavenumber.

The GTD/UTD expression is valid for a finite number of rays that pass through the observation point. When $s=-\rho_1$ or $s=-\rho_2$ the number of rays is infinite and the GTD does not give valid results. They are the caustics (see Figure 1).

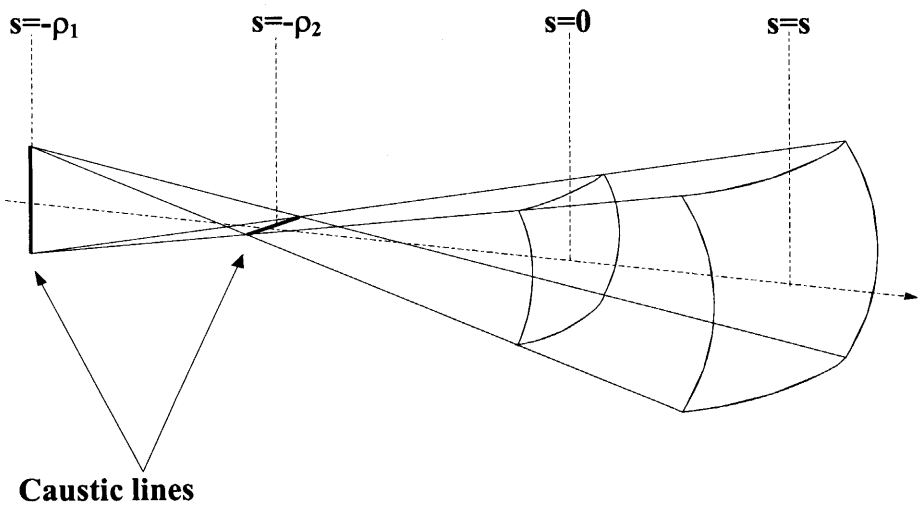

Figure 1. Astigmatic wavefront.

To apply the expression seen above the incident field shall be ray-optical [6]. In the mobile communication context, the above condition is satisfied except in certain special cases.

2.1. DIRECT FIELD

The electric field due to the direct ray is evaluated considering that the caustic lines degenerate at the same point, so the wavefront is spherical, and this point is taken as the reference point. Then applying the expression (2) the direct field is given by:

$$\vec{E}(r,\theta,\phi) = \vec{E}_t(\theta,\phi)\frac{\exp(-j\beta r)}{r} \tag{3}$$

where $\vec{E}_t(\theta,\phi)$ can be obtained from the radiation pattern of the transmitter antenna $\vec{E}_0(\theta,\phi)$:

$$\vec{E}_t(\theta,\phi) = \sqrt{\frac{\eta P_r G}{2\pi}}\vec{E}_o(\theta,\phi) \tag{4}$$

- η is the free space impedance
- P_r is the power radiated by the transmitter
- G is the gain of the transmitter antenna

These expressions can be used when the observation point is in the far-field from the antenna, as is usual in mobile communications.

2.2. REFLECTED FIELD

When the environmental obstacles are flat facets and the GO is applicable, a more efficient way to compute the field contribution of the reflected rays can be used instead of the general expression of GTD for the reflected field calculation. The method consists in applying the Image Theory and the Fresnel reflection coefficients.

Figure 2 shows a reflection case. The facet belongs to a body whose permittivity, conductance and permeability are defined by parameter ε, σ and μ respectively.

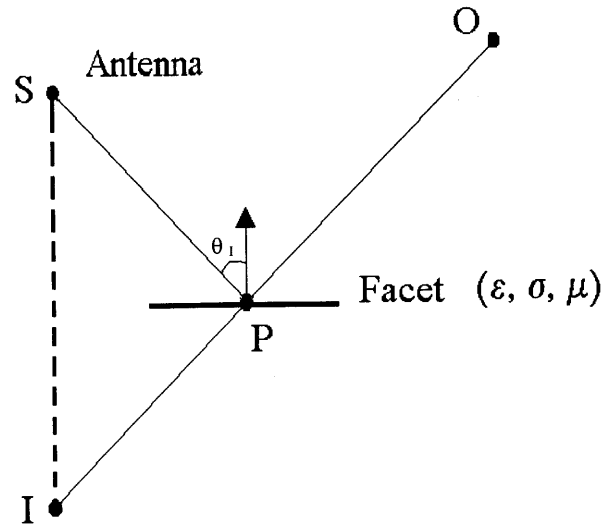

Figure 2. Transmitter antenna in front of a flat facet and definition of the image point, the reflection point and the incident angle.

According to the Snell's law the incident ray is reflected in the specular direction. It can be observed that point P can be also obtained as the intersection between the straight line IO and the facet, being the Image of the source point S.

The reflected field at point P can be obtained from the incident field using the Fresnel reflection matrix $\overline{\Gamma}$

$$\vec{E}^r = \overline{\Gamma}\vec{E}^i \tag{5}$$

where $\vec{E}^i$ can be obtained from the radiation pattern of the antenna considering an equivalent antenna at the image point I [7]. This expression can only be applied when $\vec{E}^i$ and $\vec{E}^r$ are resolved into their parallel and perpendicular components to the planes of incidence and reflection respectively. In this situation, expression (5) can be written as follows

$$\begin{bmatrix} E_{||}^r \\ E_{\perp}^r \end{bmatrix} = \begin{bmatrix} \Gamma_h & 0 \\ 0 & \Gamma_s \end{bmatrix} \begin{bmatrix} E_{||}^i \\ E_{\perp}^i \end{bmatrix} \tag{6}$$

where Γ_s and Γ_h are the so-called soft and hard reflection Fresnel coefficients [8] respectively.

The Fresnel coefficients are given by:

$$\Gamma_s(\theta) = \frac{\cos(\theta) - \sqrt{\varepsilon_r - sin^2(\theta)}}{\cos(\theta) + \sqrt{\varepsilon_r - sin^2(\theta)}} \tag{7}$$

$$\Gamma_h(\theta) = \frac{\varepsilon_r \cos(\theta) - \sqrt{\varepsilon_r - sin^2(\theta)}}{\varepsilon_r \cos(\theta) + \sqrt{\varepsilon_r - sin^2(\theta)}} \tag{8}$$

where θ is the angle of incidence formed by the incident ray and the normal vector to the facet (see Figure 2). ε_r is the complex relative dielectric constant

Thus it can be stated that the reflected field is equivalent to the direct field of an antenna whose radiation pattern is calculated as the image of the pattern of the transmitter antenna.

2.3. EDGE-DIFFRACTED FIELD

The field diffracted by an edge is given by [8]

$$\vec{E}^d(s) = \vec{E}^i(Q_d)\, \overline{D} \sqrt{\frac{\rho_e^i}{s(\rho_e^i + s)}}\, e^{-j\beta s} \tag{9}$$

where $\vec{E}^i(Q_d)$ is the incident field at the diffraction point Q_d, $\overline{D}$ is the diffraction coefficients matrix, and s is the distance between the observation point and the diffraction point.

When the field is resolved into the parallel and the perpendicular components, the dyadic form of the diffraction coefficients can be expressed as:

$$\overline{D} = \begin{bmatrix} -D_s & 0 \\ 0 & -D_h \end{bmatrix} \tag{10}$$

where D_s and D_h are the soft and hard diffraction coefficients, which can be obtained from the reflection coefficients given by:

$$D_{s,h} = D_1 + D_2 + R_{s,h}(D_3 + D_4) \tag{11}$$

where D_1, D_2, D_3 and D_4 are the components of the diffraction coefficients [9].

2.4. MULTIPLE-EFFECTS

In complex environments such as urban and indoor scenarios, multiple effects must be included to give an accurate estimation of the field at the observation points. In microcells and picocells two or three interactions are sufficient to provide a good prediction, but in large cells, sometimes it is necessary to consider higher order field contributions. A multiple effect contribution can be obtained as a combination of simple effects.

3. RAY TRACING TECHNIQUES

In a mobile communications problem, the field is calculated at a large number of observation points (thousands or even greater). Considering a faceted model for an urban environment with N_f facets, N_e edges and N_o observation points, if a "brute force" method is used, the number of intersection tests are proportional to $N_0 N_f (N_f+N_e)^X$ where X is the order prediction.

A typical microcell can be modeled by a number of facets and edges of the order of magnitude of several hundreds, so the number of intersection tests required for the ray-tracing are incommensurate. For these cases, it is necessary to reduce this number using ray-tracing acceleration techniques. The efficiency of a GTD based tool depends highly on the ray tracing simulator.

3.1. SPACE VOLUMETRIC PARTITIONING (SVP).

One of the earliest techniques used to speed up the ray tracing was the Space Volumetric Partitioning (SVP). This technique is based on dividing the space in volumes called voxels. The voxels are cubes in the three directions of the space. A 2D example is shown in Figure 3.

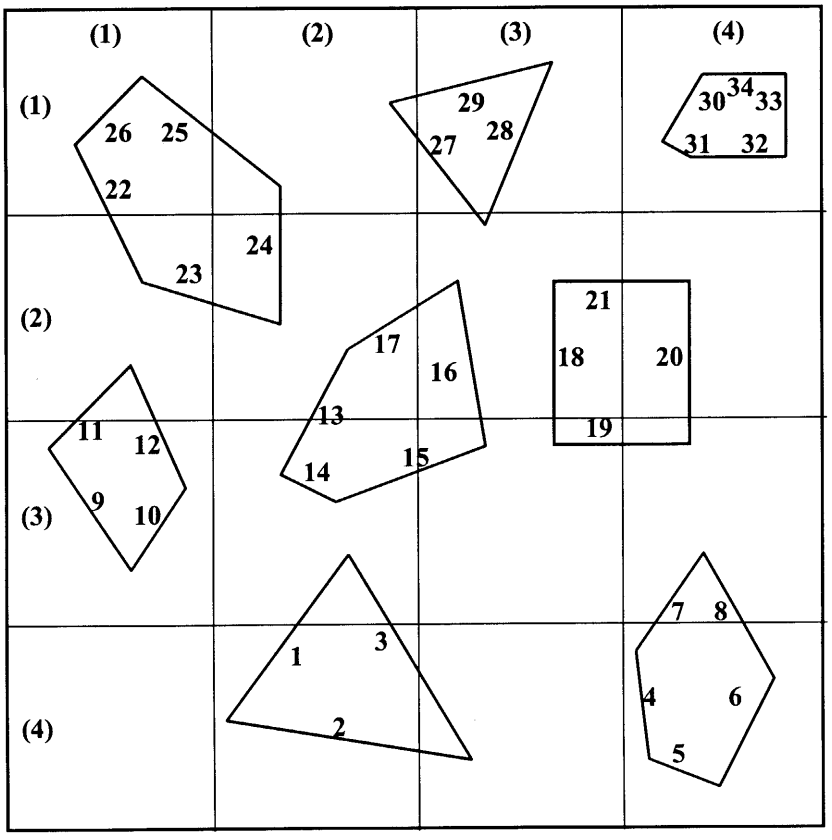

Figure 3. Example of space volumetric partitioning.

Once the space is divided, the facets that belong to each voxel are obtained, which are those that are totally or partially inside the volume. This information is loaded in the SVP matrix. The SVP matrix for the example of Figure 3 is shown in Table 1.

Voxel	Facets
(1,1)	22,25,26
(1,2)	24,25,27,29
(1,3)	27,28,29
(1,4)	30,31,32,33,34
(2,1)	11,12,22,23
(2,2)	13,17,23,24
(2,3)	16,17,18,21,27,28
(2,4)	20,21
(3,1)	9,10,11,12
(3,2)	1,3,13,14,15
(3,3)	15,16,18,19
(3,4)	7,8,19,20
(4,1)	
(4,2)	1,2,3
(4,3)	2,3
(4,4)	4,5,6,7,8

Table 1. Voxels distribution of the facets of the model.

When a shadowing test for a ray path source-observer is achieved, the voxel where the source lies is determined and all the facets loaded in the SVP matrix for this voxel are interrogated. If none of them shadows the ray, the facets contained in the next voxel that the ray crosses are considered for the intersection test. The procedure is repeated until a facet of the model shadows the ray or until the observation point is reached (in this case the ray is not shadowed and contributes to the total field).

In Figure 4, two examples of rays are shown, one shadowed and the other not. The ray from the source (S) to the first observation point (O_1) crosses the voxels (3,2), (3,3) and (3,4). Therefore, the facets loaded in these voxels must be interrogated, that is to say, the facets 1, 3, 13, 14, 15, 16, 18, 19, 7, 8 and 20 in that order. On the other hand, the ray which goes from S to the second observation point (O_2) crosses the voxels (3,2), (2,2), (2,1) and (1,1) and the facets 1, 3, 13, 14, 15, 17 and 23 should not be interrogated because this the ray is shadowed by facet number 23

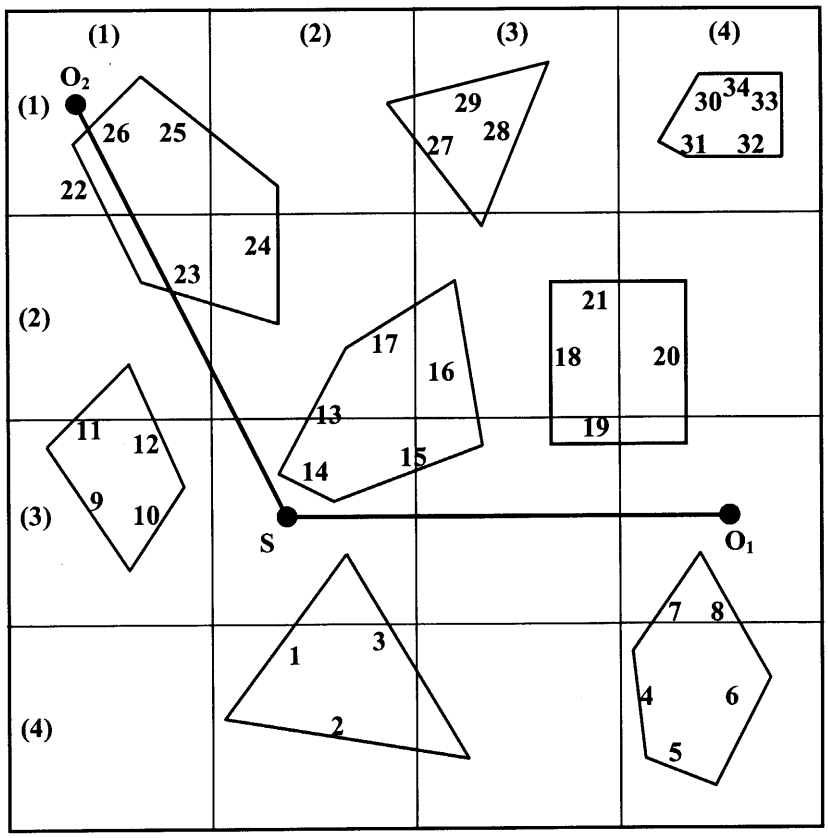

Figure 4. Example of ray tracing for two observation point.

The SVP algorithm is applied in the same way independently of the effect considered, because the source can be the transmitter antenna or a reflection, transmission or diffraction point and the observer can be an observation point or also a reflection, transmission or diffraction point. In this way the division in voxels is the same for all the effects. The only thing different is the number of paths to analyze: two if it is a simple effect, three if it is a double effect and so on. For example, for a reflection-diffraction, one starts from the transmitter antenna and questions the facets of all the voxels that the ray passes through until the reflection point is reached. Then the process is repeated from the reflection point to the diffraction point and finally from the diffraction point to the observation point. The SVP matrix only depends on the geometrical model not on the source position and the effect considered.

3.2. BINARY SPACE PARTITIONING (BSP).

The Binary Space Partitioning (BSP) [10] is a very effective technique, which takes into account the relationships between the facets of the model. For that, a BSP tree of the scene is generated: this is a binary tree, independent of the source and observer positions, which simplifies the number of facets to be interrogated to determine if the ray is or is not shadowed.

To generate the BSP tree of the model a facet of it is chosen as root and the space is divided in two regions: one formed by all the facets behind the root and the other by all which are in front of it. Each half-space will correspond with a tree branch. After that, the procedure is repeated for each branch, choosing any facet, dividing the space in two and forming other two tree branches. This procedure is repeated successively until only one facet hangs from each branch.

As an example, the BSP tree of the 2D scenario of Figure 5 is going to be generated. The procedure is the following: facet 1 is taken as root, so the plane which contains this facet, divides the space in two halves, which correspond with the tree branches. The half in front of facet 1 (according to the outward normal vector) will be on the left of the tree and the half behind on the right. The process is repeated for the facets 5 and 4 in such way that each one of the previous branches is divided again. Following the procedure recursively the binary tree is built. Figure 6 shows graphically the process.

Depending on the facet chosen, different trees of the same scene can be created. The algorithm efficiency will depend on the tree structure. The optimum tree is that which uses the least number of divided facets and tree levels. Figure 7 shows another example of BSP tree for the scenario of Figure 5. Although the number of tree levels is 5 as in the previous one, this is a better tree than the other, because it does not divide any facet. The minimum number of tree levels in a scenario is $\text{int}(\log_2 N) + 1$ where N is the number of facets. In the example the minimum number of levels would be 4.

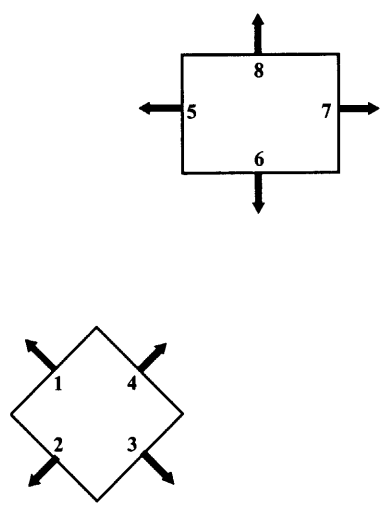

Figure 5. Scenario analysed.

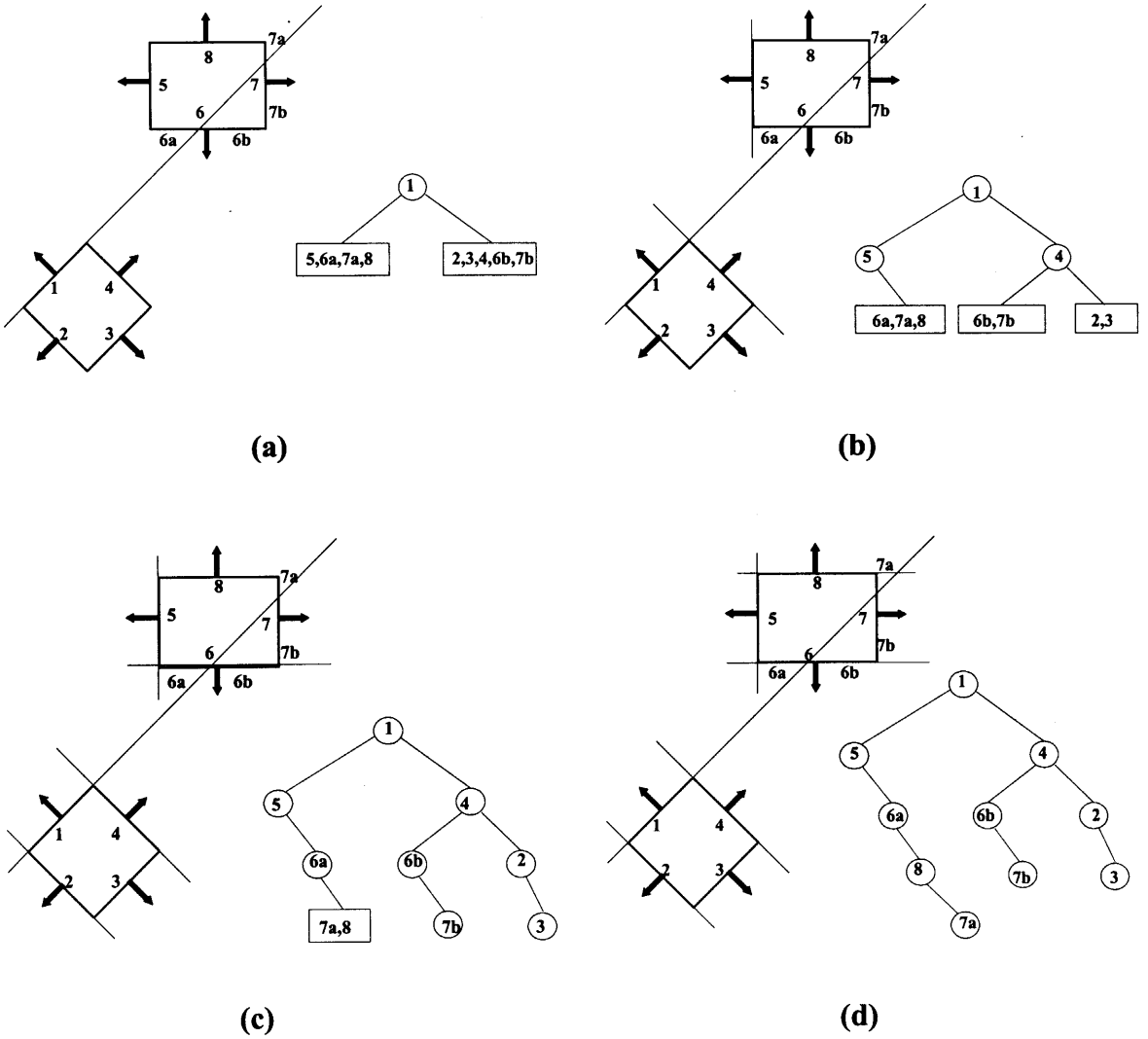

Figure 6. Binary tree generation.

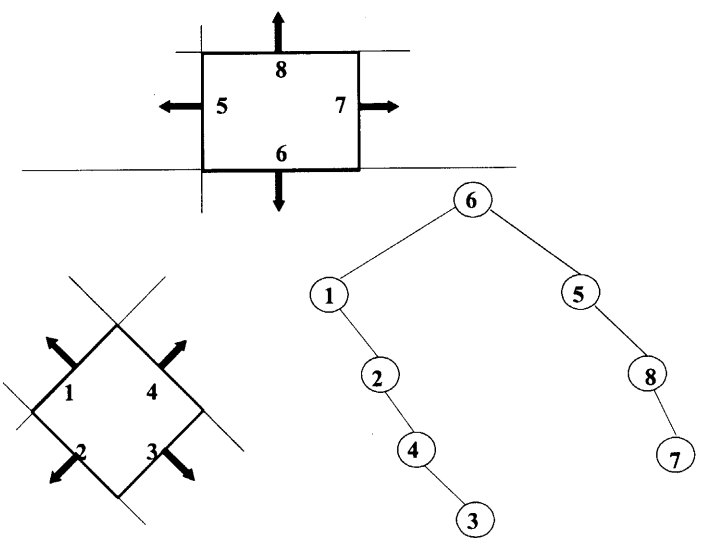

Figure 7. Binary tree from facet 6.

To interrogate the tree, one starts from the source to the observation point and there are three possible situations:

1) The source and the observation point are in front of the root facet: in this case the root facet and those which are behind it (right branch in the example) can not hide the ray.

2) The source and the observation point are behind the root facet: in this case the root facet and the facets which are in front of it (left branch in the example) can't hide the ray.

3) The source and the observation point are in different half-spaces: then the root facet can hide the ray and the intersection test must be done rigorously.

In cases 1 and 2 all the facets placed in a half-space of the model are discarded and the analysis must be continued for other branch of the tree.

As in the SVP algorithm, the BSP tree creation does not depend on the effect considered, only change the number of times that the tree must be questioned which will depend on the number of stretches of the ray, or, what is the same, on the effect is being treated.

3.3. THE ANGULAR ZETA BUFFER (AZB) ALGORITHM

The AZB technique has been developed by the authors. It is based on the Light Buffer technique [11] used for computer graphic design. The AZB has a lot of particular features that make it especially well suited for the UHF propagation problem, especially for the treatment of diffraction. The application of the algorithm is different for each coupling mechanism considered, as discussed in the following subsections.

3.3.1 Application to direct rays

For the direct ray case, the space is divided into spherical sectors from the source point called anxels. They are defined by the spherical coordinates theta (θ) and phi (ϕ) of a fixed coordinate system located on the source (see Figure 8).

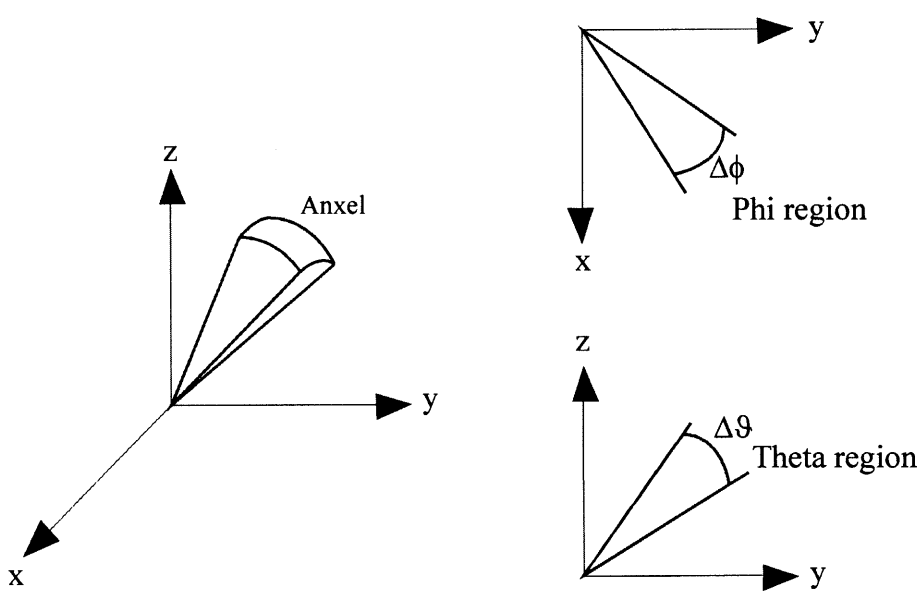

Figure 8. Anxel definition.

The anxel where each facet belongs is computed from the spherical coordinates of its vertices. Figure 9 shows a representation of the anxels in the θϕ plane (AZB plane), with an example of facets that lie in each anxel

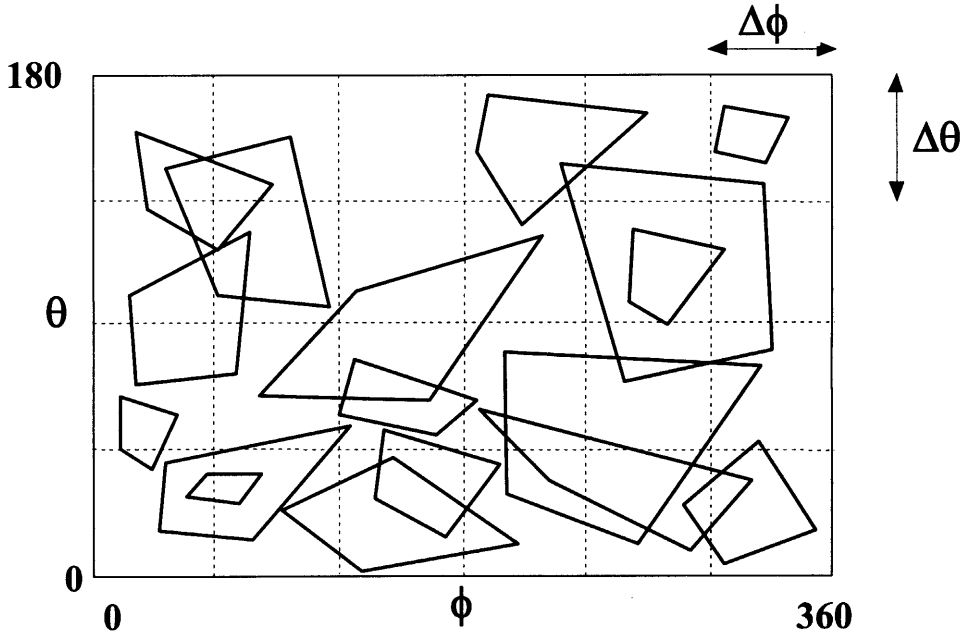

Figure 9. Facets' storage in the AZB plane.

This information is stored in the so-called AZB matrix. It depends, exclusively, on the source point and on the environmental model. For each anxel the facets are arranged according to the distance to S. As an example, Figure 10 shows the simple 2-D outdoor scene of Figure 3 where a space partitioning in 12 anxels has been accomplished. Table 2 shows the storage of the facets in the AZB matrix.

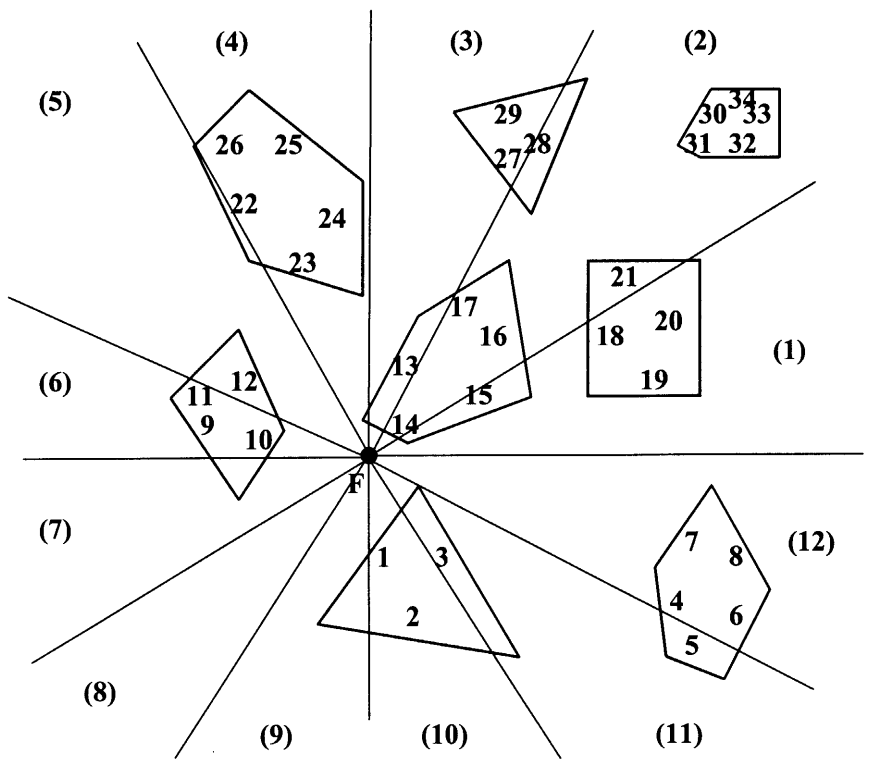

Figure 10. Example of a 2-D outdoor scene divided in 12 "anxels".

Anxel	Facets
1	14,15,16,18,19,20,21
2	14,16,17,27,28,18,21,31,32,30,33,34
3	14,13,17,27,29
4	14,13,23,24,25,26
5	12,11,23,22,26
6	10,12,9,11
7	10,9
8	
9	1,2
10	1,2
11	1,3,2,4,5,6
12	4,7,8,6

Table 2. Facets storage in the AZB of the scene of Figure 14

In outdoor scenes, only illuminated facets from the source are taken into account. To know if a facet is illuminated, the backface culling test is applied (see Figure 11) and the facets which are not illuminated are removed of the AZB matrix. For example, in anxel 1, facets 16, 20 and 21 can be removed. Also, there can be facets shadowed by others closer to the source (eclipse shadowing). All the facets totally shadowed are removed from the AZB matrix. For example in anxel 2 facets 18, 21, 27, 28, 31, 32, 30, 33 and 34 are totally shadowed by facet 14.

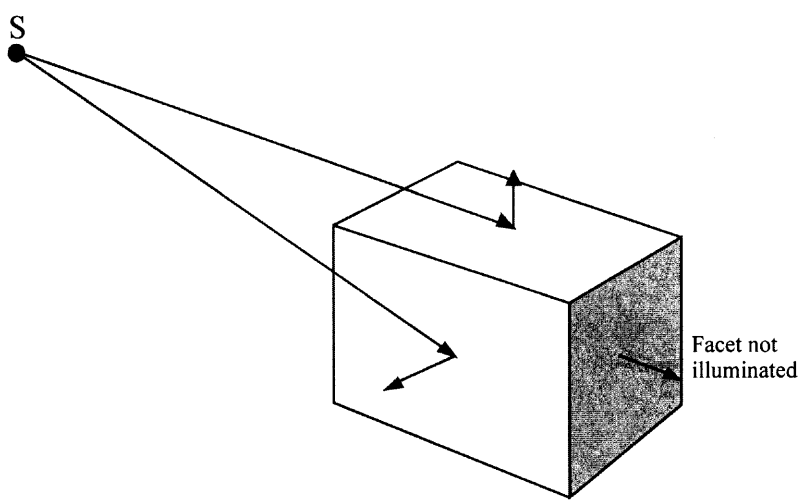

Figure 11. Application of the backface culling test.

To make the shadowing test for a given observation point (O), this is located in the corresponding anxel by means of their spherical coordinates. Then the facets placed in the anxel with distance to S less than the distance S-O are required. Figure 12 shows a case with two observation points. The point O_1 is in anxel 1 and only the facets 14, 15, 18 and 19 are interrogated, because the others are not illuminated. In this case any facet does not obstruct the ray. The point O_2 is in anxel 4, the intersection

test is made with facets 23 and 24 (the only ones illuminated in the anxel). It can be observed that the ray is shadowed by facet 23

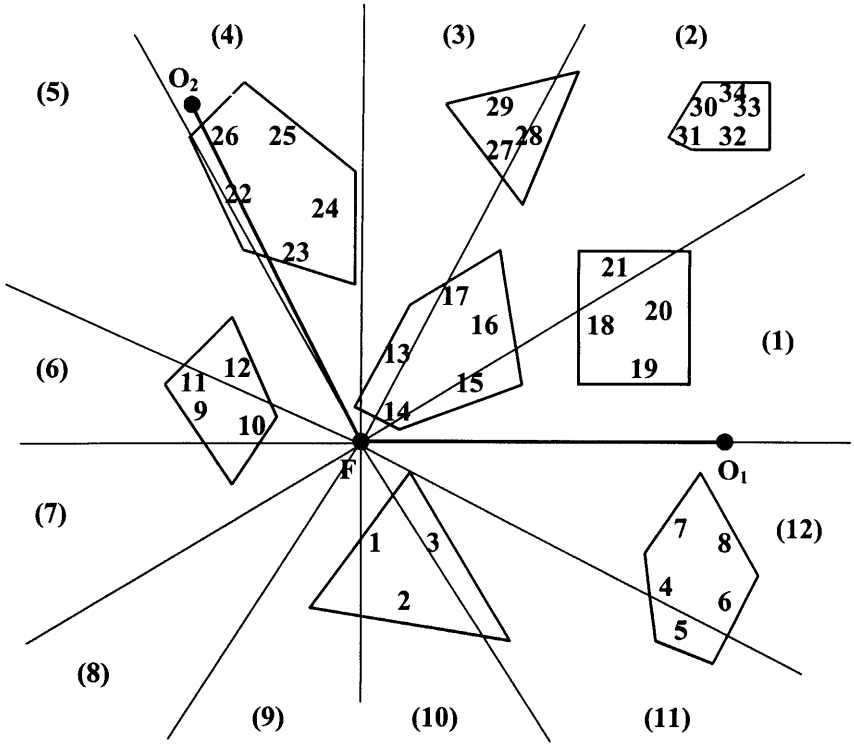

Figure 12. The shadowing test for two observation points.

The reduction in the number of facets tested decreases with the number of anxels, that is to say, it depends on the values of $\Delta\theta$ and $\Delta\phi$. On the other hand, the number of regions is limited by the memory size available.

3.3.2 Application to reflected rays

The algorithm application is similar to the direct ray case taking, in this case, as sources the images (I) of the transmitter antenna (S) with respect to the directly illuminated facets. It is taking into account that each image only radiates in the reflection space (RS) (see Figure 13). Therefore, the space to divide in anxels is limited by the highest and lowest values of the spherical coordinates (θ, ϕ) of the reflecting facet vertices.

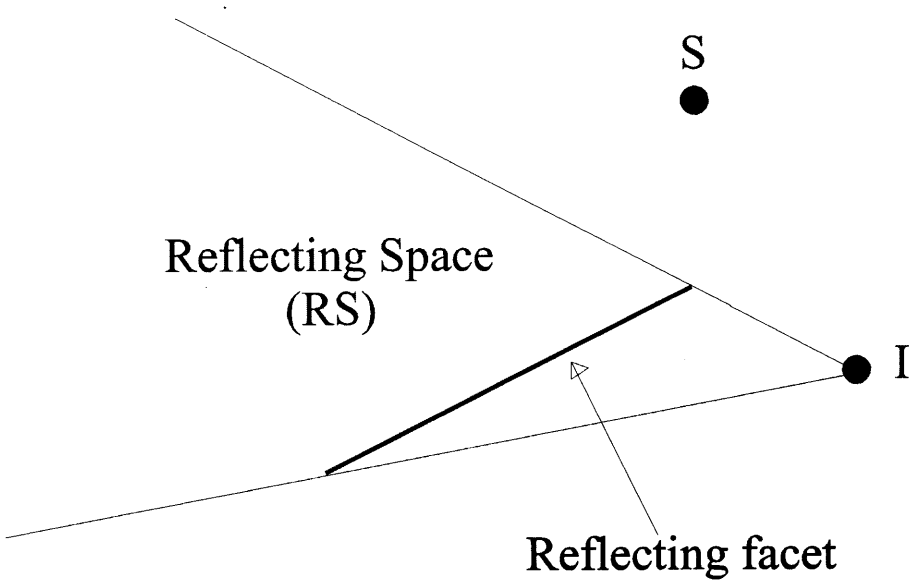

Figure 13. Reflection space (RS)

For the shadowing test, the first thing is to calculate if the observation point (O) is into the reflection space. If this condition is satisfied, it is found the anxel where this point is placed. Finally, the facets located on the anxel are tested orderly, following the same procedure as in the direct ray. The analysis of the incident ray (from S to the reflection point) is done using the AZB matrix of the direct field, taking the reflection point as the observation point.

3.3.3. Application to edge diffracted rays

Given a source (S) and an edge, the coordinates β, α are used instead of the spherical coordinates θ, ϕ. These coordinates are defined as follows: β is the angle of the Keller's cone for a diffraction point and α is the angle formed by the diffracted ray and the first facet of the wedge (see Figure 14). So, the facet arrangement is accomplished in terms of these coordinates. For each source-edge pair the space where diffracted rays can exist is limited by the edge coordinates ($\beta_{\max}, \beta_{\min}, \alpha_{max}, \alpha_{\min}$) which fix the margins of the so-called AZB rectangle of diffraction. This rectangle is divided into anxels.

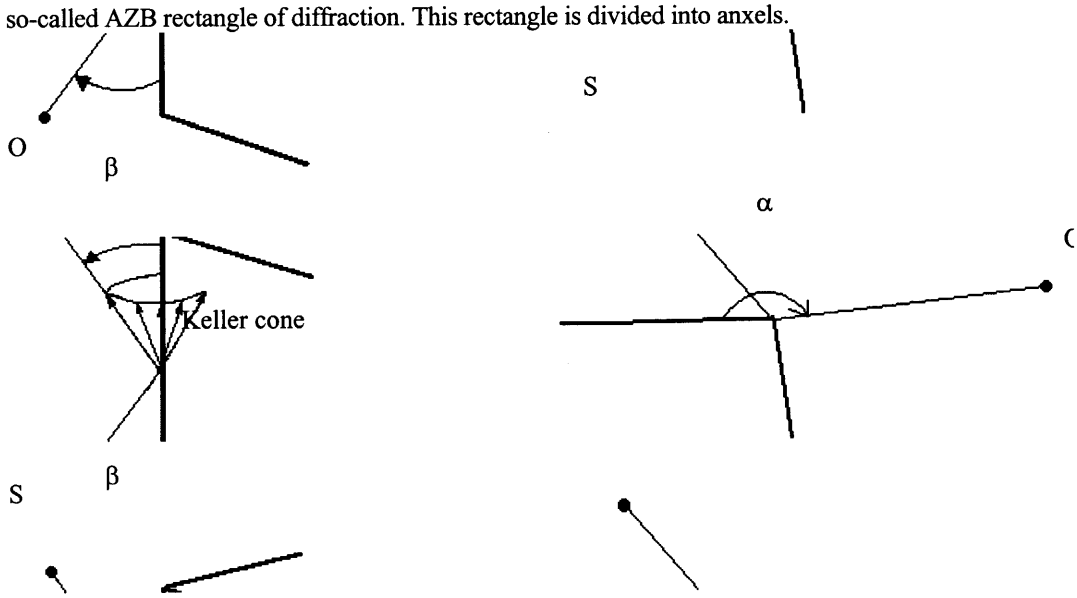

Figure 14. Definition of the β and α angular parameters for the AZB of edge-diffraction

The facets of the environment are located in the anxels of the AZB rectangle by means of the edge coordinates of their vertices. This information is stored in the so-called AZB matrix of diffraction. Given an edge and an observation point, its edge coordinates (β_o, α_o) are computed and, if they are into the rectangle margins, the anxel where the point lies is determined. Only the facets stored in the cell are considered in the test of the diffracted ray shadowing. If the diffracted ray is not hidden, the incident ray (source-diffraction point) is analyzed. To complete this task, the AZB matrix of the direct field is used, taking the diffraction point as the observation point.

3.3.4 Application to multiple effects

For multiple effects, the ray-tracing is made as a combination of the effects involved using the information of the corresponding AZB matrices. For instance, for reflection-diffraction, first the reflection and diffraction points are computed, and after this the intersection test for every path is made. For the diffraction the AZB matrices created from the edge are employed, for the reflection the AZB matrices of reflection are used, and, finally, for the incident ray the AZB matrices of direct ray are considered.

3.4. COMPARISON BETWEEN THE DIFFERENT ACCELERATION RAY-TRACING TECHNIQUES.

The BSP technique is very efficient for 2D scenes where making the BSP tree is relatively easy. However for 3D scenarios this task is more complex, it being difficult to find an optimum tree. Often, the trees are very long and with lots of broken facets, resulting trees which are not useful for efficient analysis.

The SVP method, for large scenes, needs a large number of voxels in order to load a low amount of facets per voxel. Also, when the source is far away from the observation point, the number of voxels that cross the ray is very high and, therefore, the amount of facets that are considered in the intersection test is enormous. In the example of Figure 3, it can be observed that the number of interrogated facets is, on average, less in the AZB method than in the SVP method.

The SVP method has the advantage of the memory size required, because it only needs a matrix that depends only on the scene, whereas the AZB technique has to make a matrix by source (antenna, image, edge, etc). For high order effects, when the number of sources is very large and the number of observation points involved in the effect is very low, it is not efficient to create the AZB matrices. In these cases the SVP method can be combined with the AZB.

The AZB technique has the advantage, with respect to the other methods, that it only load the facets not shadowed by illumination or by eclipse, because the space is divided taking the source as reference. This allows a reduction in the number of facets stored in each matrix.

4. RESULTS

In this section, validation of GTD/UTD approach using the AZB technique, is presented for two kinds of scenarios: an urban environment and an indoor environment.

For the urban environment, a Manhattan scenario has been analyzed, as shown in Figure 15. For this case, three paths along three streets have been simulated and compared with measurements [12]. In Figure 15 the antenna position and the three paths can be observed. Path 1 is along 51st Street (1200 m), path 2 is along Lexington Avenue (1300 m) and path 3 is along Third Avenue (1300 m).

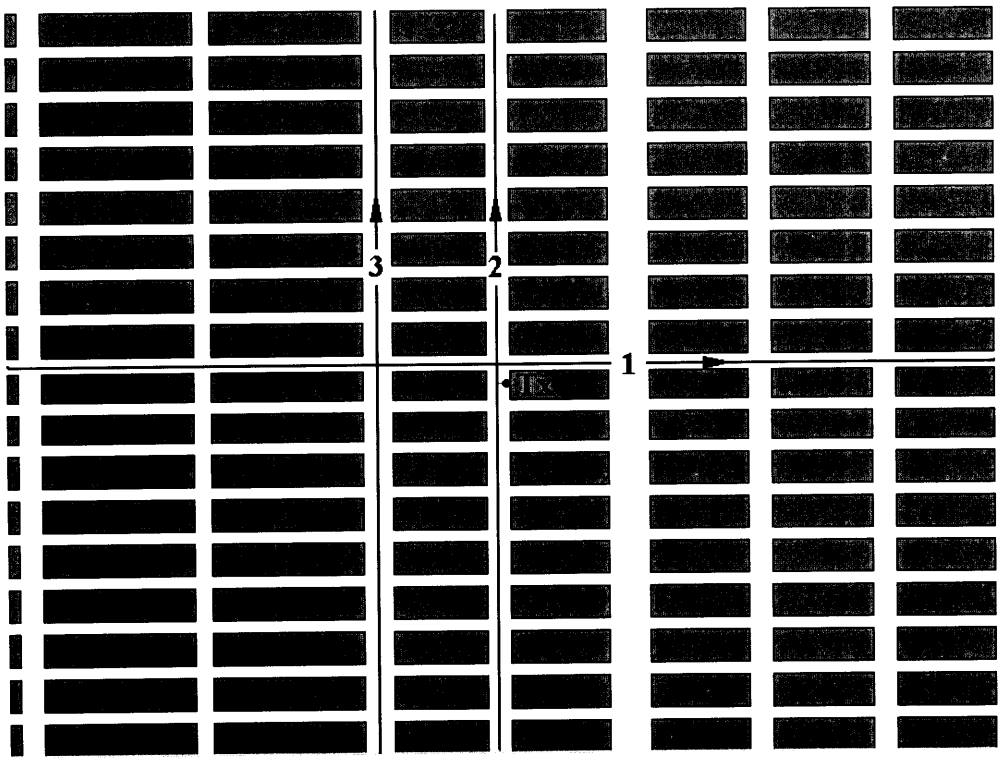

Figure 15. Plant view of Manhattan scenario with antenna position (Tx) and paths 1,2 and 3 analyzed (taken from [7]).

This scenario has been modeled with 680 facets and 1,888 edges. The electric properties of the facets are: ε_r=15, μ_r=1, and σ=7 S/m. This environment has been simulated using a code called FASPRO, which has been developed by the authors. This code, based on GTD and on the AZB acceleration ray-tracing technique, allows analysis of propagation in outdoor environments. Prediction path loss results, compared with measurements, are shown in Figures 16 to 18. In the x-axis the distance in meters is represented, taking the source as reference. The mechanisms considered are first-order effects, second-order effects (except double diffractions), and third-order effects, which involve a ground reflection and do not involve more than one diffraction.

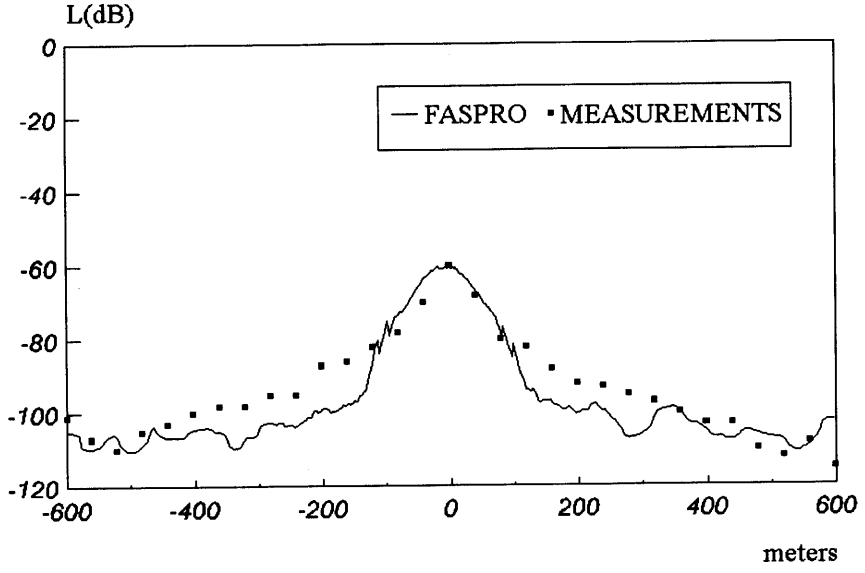

Figure 16. Comparison between measurements and computations of path 1 (taken from [7]).

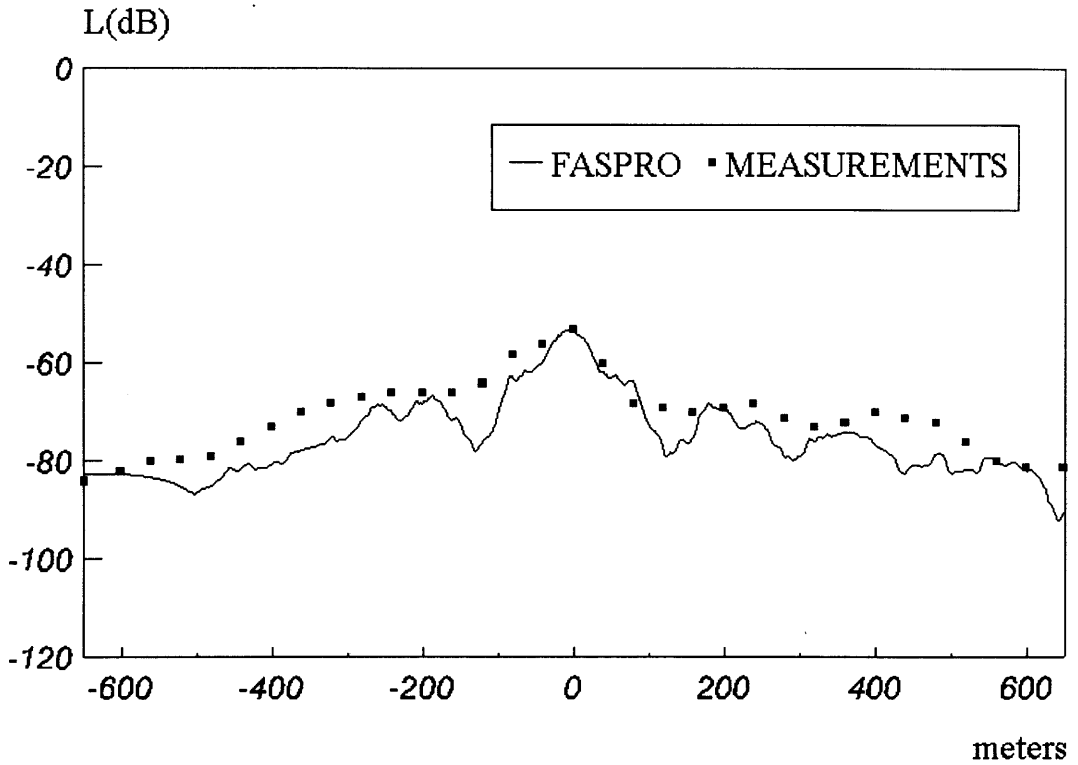

Figure 17. Comparison between measurements and computations of path 2 (taken from [7]).

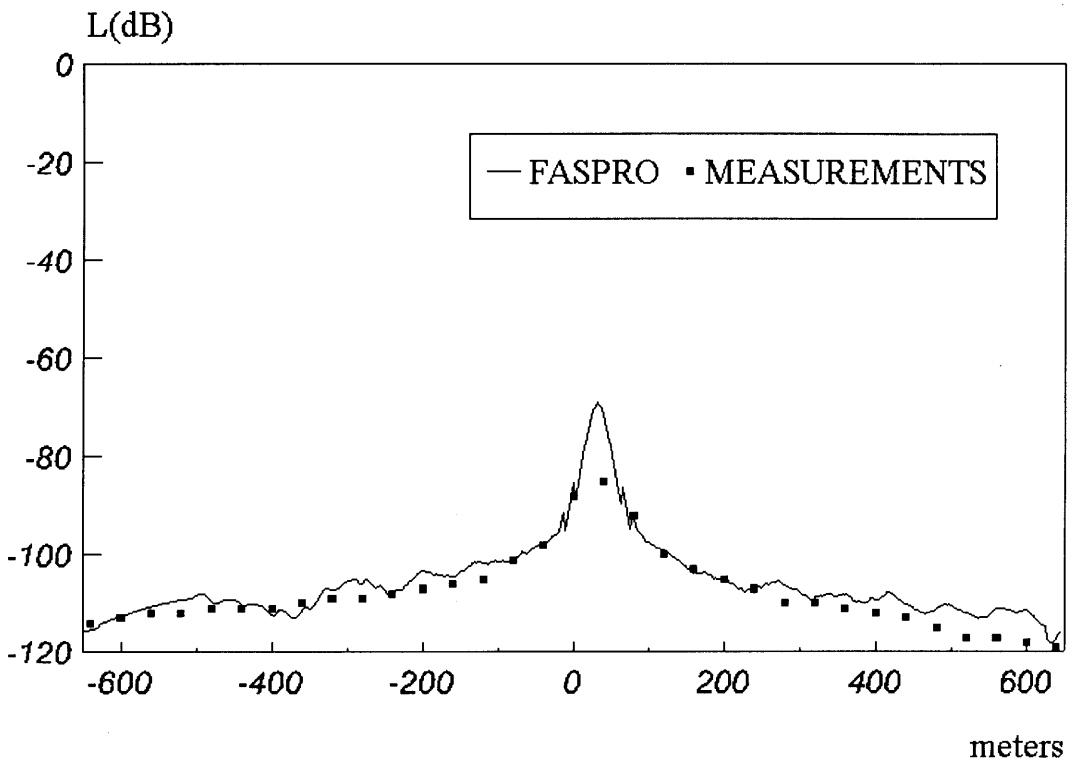

Figure 18. Comparison between measurements and computations of path 3 (taken from [7]).

It can be observed that the agreement between measurements and simulation results is good for engineering purposes. Table 3 shows the CPU time necessary to analyze each path on a Pentium 333 MHz with 128 MB of RAM. It can be seen the high efficiency of the method.

Caption Path	Distance (m)	Number of points	Time
1	1200	1200	5'44"
2	1300	1300	5'58''
3	1300	1300	6'01"

Table 3. CPU time for the three paths in Manhattan.

For the indoor environment, the office scenario shown in Figure 19 has been analyzed. Measurements were made and compared with simulation results. A code, called FASPRI, which has also been developed by the authors, has been used for the simulation. This code is based on GTD and on the AZB acceleration ray-tracing technique and has been designed to analyze the indoor propagation. The antenna position and orientation and the paths analyzed are shown in Figure 19. In the first path the measurements were made at 48 points. The path length is 20.1 m. The second path is 28.3m long and the measurements were done at 74 points. Path 3 is 20.3 m long and the measurements were made at 48 points.

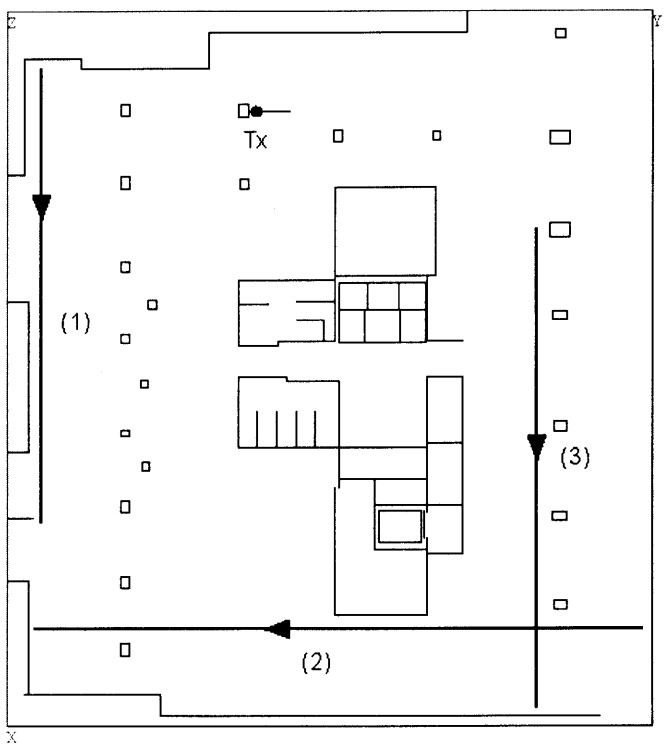

Figure 19. Plan view of the indoor scenario analyzed with the antenna position and the paths to simulate.

This scenario has been modeled with 175 facets. In the simulation all the facets have the same electric properties: ε_r=4.44, μ_r=1.0, σ =0,08 S/m and the same width: 0.1m. The mechanisms considered were: simple effects, double effects, triple reflections, third-order effects involving one, two or three

transmissions and fourth-order effects involving two, three or four transmissions. Predictions compared with measurements are shown in Figures 20 to 22 (paths 1 to 3).

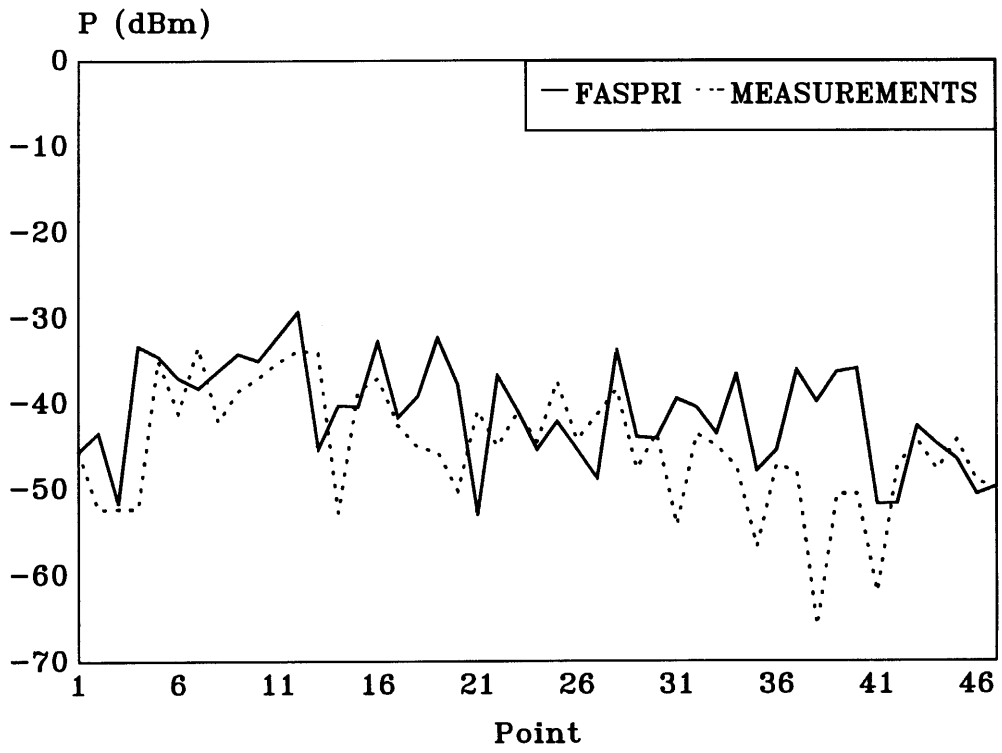

Figure 20. Comparison between measurements and computations of path 1

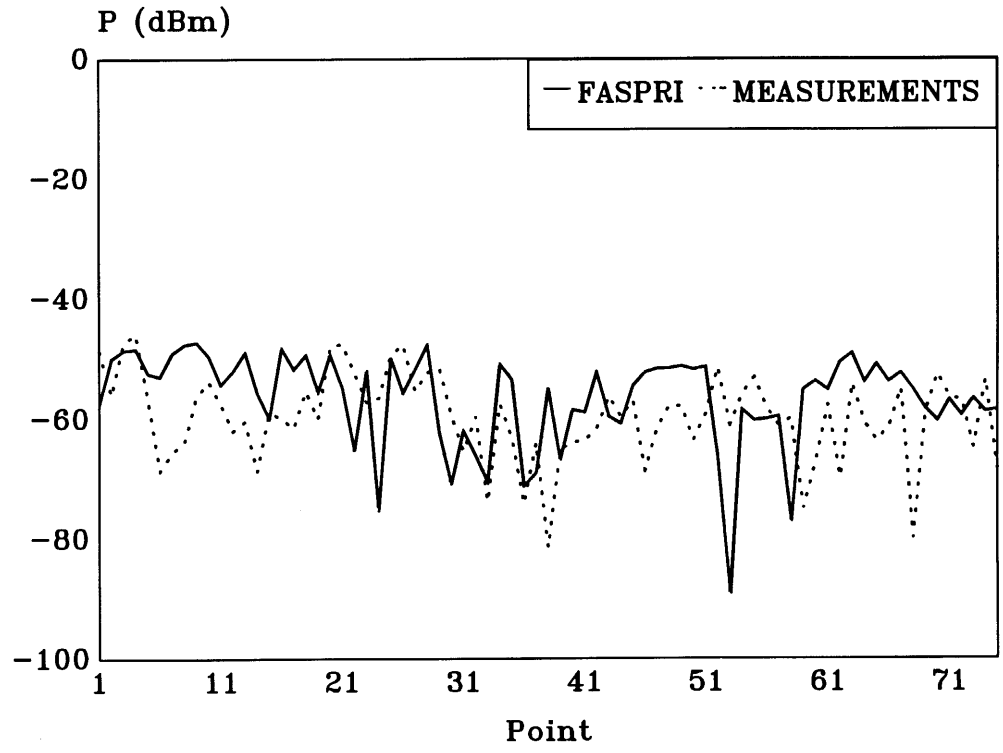

Figure 21. Comparison between measurements and computations of path 2

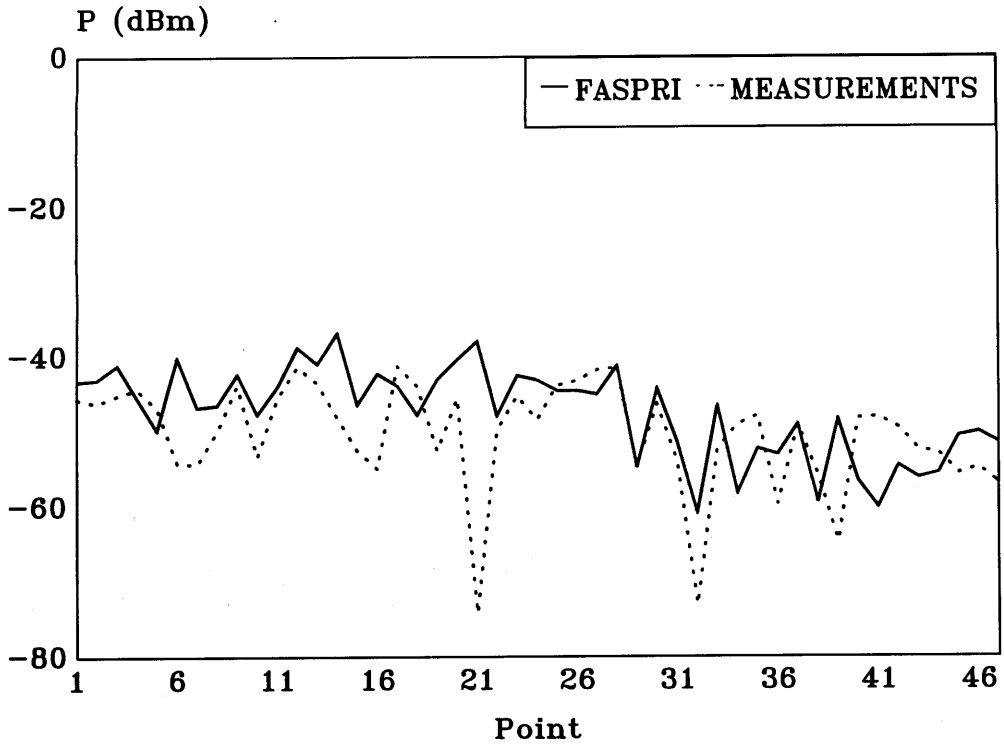

Figure 22. Comparison between measurements and computations of path 3

Other measurements were made with the same antenna placed on the ceiling pointing to the floor. Figure 23 shows the new antenna position and the paths analyzed. Path 4 is 25.7 m long and the measurements were made at 68 points, whereas path 5 is 14.8 m long and the measurements were made at 21 points. The same mechanisms were considered. Figures 24 (path 4) and 25 (path 5) show the comparison between these measurements and simulation results

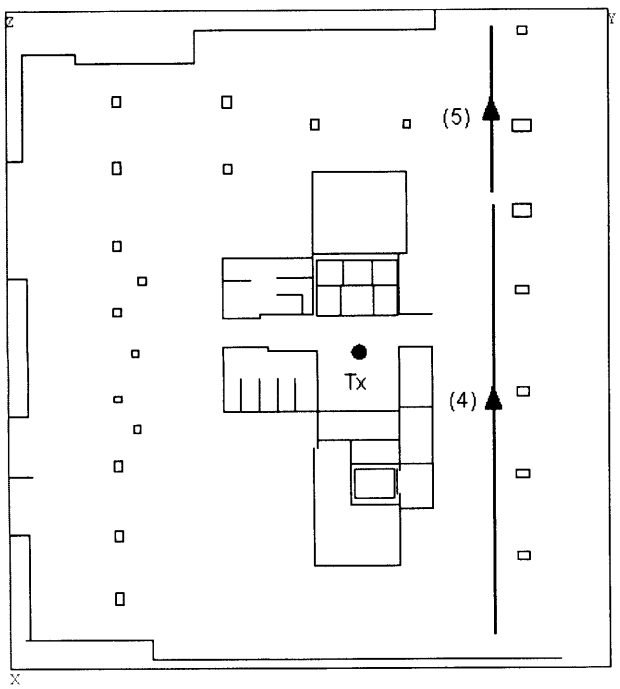

Figure 23. Plan view of the indoor scenario analyzed with the antenna position and the paths to simulate.

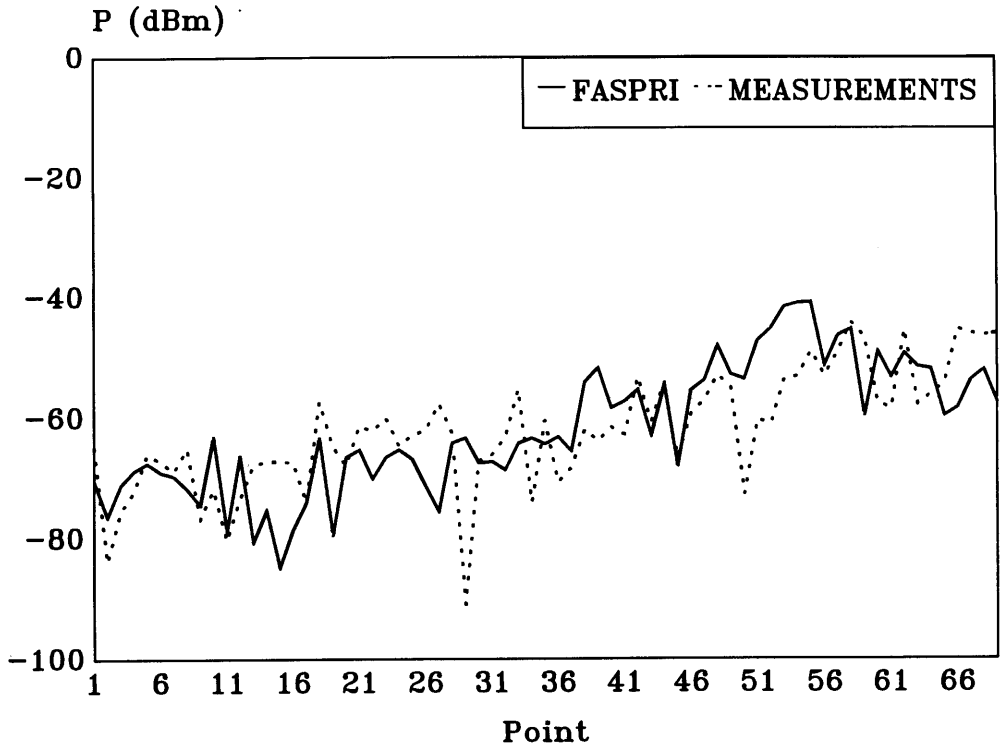

Figure 24. Comparison between measurements and computations of path 4

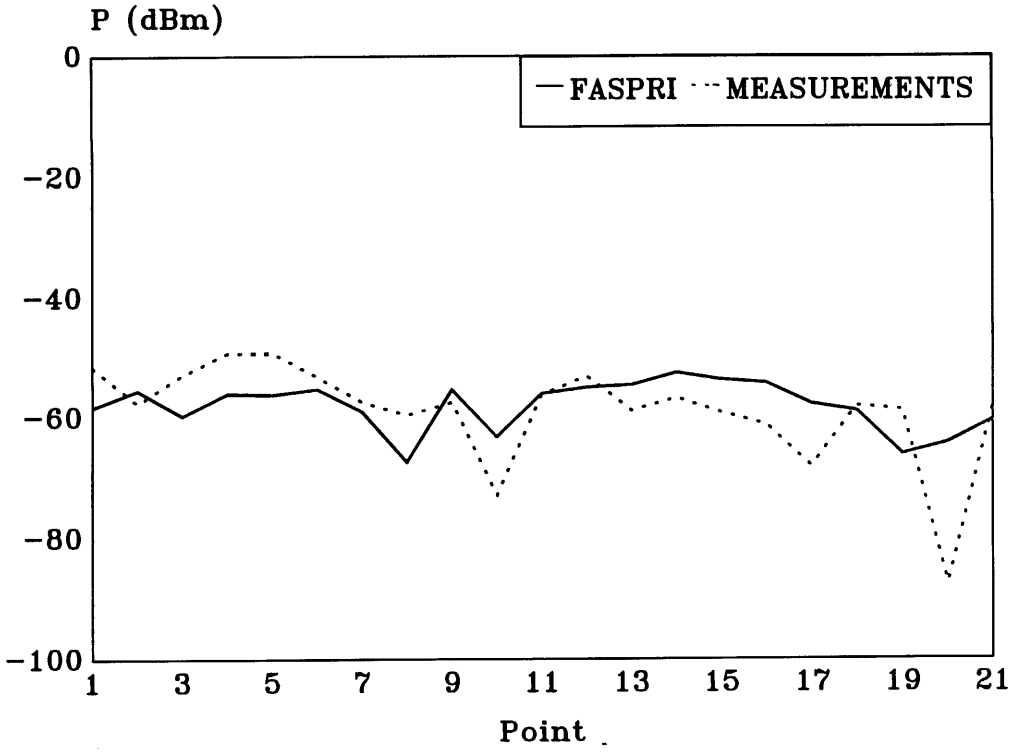

Figure 25. Comparison between measurements and computations of path 5

As in the outdoor case, predicted values are deemed reliable for engineering design. Table 4 shows the computation time necessary to obtain the results of each path in the same computer described above. It can be noticed that, on average, this method consumes 8" of CPU time for each point analyzed, what proves its efficiency.

Caption Path	Distance (m)	Number of points	Time
1	20.1	48	5'45''
2	34.7	74	9'34''
3	20.3	48	5'51''
4	25.7	68	8'42''
5	14.8	21	2'33''

Table 4. Computation time of the different paths in the indoor environment.

5. CONCLUSIONS

Some acceleration ray-tracing techniques have been presented for a propagation model based on GTD/UTD techniques for mobile communications. The Angular Z-Buffer method has been implemented, which allows the realization of the propagation model in a PC with low cost in time. This method has been validated with measurements for urban and indoor scenarios, obtaining good accuracy.

6. REFERENCES

[1] D. Parsons, *"The mobile Radio Propagation Channel"*, London, Pentech Press Limited, 1992

[2] Glassner, A. S. (Ed.) *" An Introduction to Ray Tracing"*, San Diego, CA: Academic Press, 1989.

[3] Foley, J. D., A. Van Dam, S. K. Feiner, and J. F. Hughes, *"Computer Graphics. Principles and Practice"*, 2nd ed., New York: Addison-Wesley, 1995.

[4] M. F. Cátedra, J. Pérez, F. Saez de Adana, and O. Gutiérrez *"Efficient Ray-Tracing Techniques for Three-Dimensional Analyses of Propagation in Mobile Communications: Application to Picocell and Microcell Scenarios"*, IEEE Antennas and Propagation Magazine, Volume 40, Nº 2, April 1998, pp 15-28.

[5] M. F. Cátedra, J. Pérez, F. Saez de Adana, O. Gutiérrez, J. Cantalapiedra, I. González *"Fast Ray-Tracing Method for Calculating the Propagation in Indoor Environments"*, IEEE Antennas and Propagation Society Intenational Symposium, Atlanta, Georgia June 21-26, Volume 3, pp 1656-1659.

[6] Mc Namara, D. A., C. W. I. Pistorious, and J. A. G. Maherbe, *"Introduction to the Uniform Geometric Theory of Diffraction"*, Norwood, MA: Artech House, 1990.

[7] M. Felipe Cátedra, Jesús Pérez, *"Cell Planning for Wireless Communications"*, Artech House, 1999.

[8] C.A.Balanis. "Advanced Engineering Electromagnetics". John Wiley and Sons, 1989.

[9] Kouyoumjian, R. G., and P. H. Pathak, *"A Uniform Geometrical Theory of Diffraction for an Edge in a Perfectly Conducting Surface"*, *Proc* IEEE, Volume 62, N° 11, Nov. 1974, pp 1448-1461.

[10] Fuchs, H., *"On Visibility Surface Generation by a priori Tree Structures,"*, Computer Graphics, Vol. 14, N° 3, July 1980, pp 124-133.

[11] Hines, E. A., and D. P. Greenberg, *"The Light Buffer: A Shadow-Testing Accelerator"*, IEEE Computer Graphics and Animation, September 1986, pp. 6-16.

[12] A.J.Rustako, N.Amitay, G.J.Owens, R.S.Roman. *"Radio propagation at microwave frequencies for line-of-sight microcellular mobile and personal communications"*. IEEE Transactions on Vehicular Technology, vol. 40, 1991, pp. 203-210.